CIMAC CONGRESS 25
ZURICH, MAY 19 – 23, 2025

2025 | 318

Research on injection volume closed-loop control based on MPC for high-pressure common rail system

Controls, Automation, Measurement, Monitoring & Predictive Maintenance

Bingxin Liu, Harbin Engineering University

Hongzi Fei, Harbin Engineering University
Liuping Wang, RMIT University
Xiongqin Li, Harbin Engineering University
Sheng Han, Harbin Engineering University
Zeyu Jing, Harbin Engineering University
Yu Ding, Harbin Engineering University

ABSTRACT

The injection performance of the fuel system plays a crucial role in determining the engine efficiency and emission performance. The high-pressure common rail (HPCR) injection technology provides a great advantage in the flexible control of the injection process with its increasingly high injection pressure and fast response. However, modern production HPCR systems adopt the open-loop control based on calibration maps to regulate the injection process. Due to the complex structure and the interplay of multiple physical fields, it is challenging to ensure the consistency of the actual injection and the desired target value, thus restricting further optimization of the combustion and emission performance. The closed-loop control of the fuel injection volume is the fundamental approach to enhance the injection control precision and eliminate disturbances. However, this control system is a multi-variable coupled system that involves multiple injectors operating in a specific timing sequence. And there exists nonlinearity between the injection pulse width control signal and injection volume under varying operating conditions. These factors bring significant challenges for the controller design. The model predictive control (MPC) is an optimal control method suitable for such complex control systems. Therefore, in this paper, a closed-loop control method based on MPC for the fuel injection volume of HPCR systems is proposed and investigated.

First, according to the influence mechanism between the injection pulse width and injection volume, a state space model of the injection control system under different rail pressure conditions is constructed. On this basis, the MPC-based controller is designed, where the impact of the weighting matrices in the objective function on the control performance is thoroughly explored. Second, to address the model nonlinearity associated with a large range variation of rail pressure and overcome the regulation limitation of the injection pulse width control signal, an adaptive optimization approach is employed in the MPC controller to enhance both the control accuracy and response characteristics. In addition, for the issue that the injection volume cannot be measured during actual operation, a real-time injection estimation method based on the Kalman filter using the measured rail pressure was designed and implemented in our previous study. Here it is successfully applied in this research, and the closed-loop control performance with the estimated injection volume as feedback is analyzed. Finally, to verify the effectiveness of the designed controller, a high-fidelity hydraulic model of the HPCR system is built using AMESim, and the MPC controller model is established in Simulink. The proposed control method is validated through the AMESim/Simulink co-simulation platform. The results demonstrate that compared to the existing open-loop control mode, the application of the method proposed in this paper exhibits a significant enhancement in the fuel injection control accuracy, with steady-state errors less than 1.5 mm3. Moreover, the injection volume is effectively controlled back to the target value within three injection cycles under disturbances.

1 INTRODUCTION

With the increasingly stringent global air pollution policies and the implementation of carbon neutral strategies, significant challenges have been brought to engine technology [1-3]. The injection performance of the fuel system plays a critical role in determining both the engine efficiency and emissions characteristics. The high-pressure common rail (HPCR) injection system, which characterized by its high injection pressure, rapid response time, and flexible injection strategies, provides crucial support for the efficient and stable operation of engines [4,5]. However, most modern HPCR systems rely on open-loop control based on calibrated MAP tables to regulate the injection process. This control method lacks real-time feedback adjustment, which limits the accuracy of fuel injection volume control [6]. During the actual engine operation, due to the complex hydraulic effect in HPCR system, changes in working environments and operating conditions, as well as the degradation of system structural parameters, it is difficult for the actual injected fuel volume to remain consistent with the target value, thus limiting the further optimization of the combustion and emission performance.

Closed-loop control of fuel injection volume is a fundamental approach to improving the injection control accuracy and eliminating the impact of disturbances. If the injection volume can be closed loop controlled directly through real-time feedback of the injection information, it will significantly enhance the precision of the fuel injection process. However, due to the complexity of the system structure and the harsh in-cylinder environment, it is challenging to measure the injection volume in real time during the actual engine operation. Currently, several researchers and injection system manufacturers have explored technologies for injection estimation and control. For example, Delphi [7] proposed a "switch" injection closed-loop strategy, where the voltage signal is monitored to determine the moments when the needle valve reaches its maximum lift and seat position. This information is then used for injection estimation and closed-loop compensation of the injection duration. Bosch [8] developed a Needle Closing Control (NCC) injector equipped with a force sensor in the control chamber to detect the needle valve closing time, thus enabling closed-loop regulation of the injection process. Ferrari et al. [9,10] installed pressure sensors on the high-pressure fuel tube between the common rail and the injector. They utilized the pressure signal to estimate the fuel injection quantity and employed a PID controller to correct the injection pulse width based on the difference between the estimated and target injection quantities, thereby achieving closed-loop control. The research on closed-loop control of fuel injection volume remains relatively limited. Most studies focus on attaching sensors inside the injector or on the high-pressure fuel tube to capture relevant information about the injection process, enabling the estimation of injection data and improving control accuracy.

Existing studies tend to modify the mechanical structure of current systems, and most are still in the exploratory phase with limited in-depth analysis of the closed-loop performance yet. Therefore, it is crucial to further investigate the injection estimation and control methods. Modern HPCR systems are already equipped with rail pressure sensors, and studies have shown that the pressure fluctuations in the common rail, caused by fuel injection, can reflect important information about the injection process [11-14]. A Kalman filter-based estimation method for injection characteristics using rail pressure has been proposed in the literature [15,16]. This method considers complex factors in practical applications, such as the measurement noise, modelling error, and model nonlinearity, enabling real-time optimal estimation of fuel injection rate and volume under various operating conditions. Based on this, the real-time estimated injection volume can be used as feedback for the closed-loop control of injection.

The addition of real-time feedback of observed fuel injection and formation of closed-loop control for fuel injection volume in existing HRCR systems will inevitably lead to the complexity of the system structure and multivariate coupling. Conventional PID control methods have a small computational requirement. However, due to the limitations of the injector actuator and the nonlinear relationship between injection pulse width and fuel injection volume under different operating conditions, it may be difficult for PID to obtain the desired control effect and robustness. Model predictive control (MPC) is an advanced control strategy well-suited for such complex systems [17]. The method features multi-step prediction, rolling optimisation and feedback correction, and can account for the effects of system constraints in the optimization process [18]. Compared to PID control, MPC has clear advantages in solving optimization problems with constraints and ensuring robustness. It has been successfully applied across various fields, including energy and power systems [19-21].

The objective of this study is to investigate the MPC-based closed-loop control for fuel injection volume in HPCR systems. First, a state space model of the fuel injection control system is established according to the mechanism of injection process. Based on this model, the fuel injection volume closed-loop controller is designed based on MPC. To address issues of model

parameter matching for large changes in operating conditions and the regulation limitations of the injection pulse width control signal, an adaptive optimization is designed and implemented within the MPC controller to ensure control accuracy and response characteristics. Finally, the anti-disturbance and robustness capabilities of the designed closed-loop control system is verified via the Amesim/Simulink co-simulation platform.

The organization of this paper is as follows: Section 2 describes the structure and working process of the fuel injection volume closed-loop control system. Section 3 establishes the fuel injection model and presents the optimal design of predictive control with constraints. Section 4 introduces the implementation process and validates the control performance of the designed fuel injection volume closed-loop controller. Section 5 summarizes the main conclusions of this research.

2 DESCRIPTION OF THE INJECTION CLOSED-LOOP CONTROL SYSTEM

In HPCR injection systems, the ECU determines the injection timing and pulse width referring to the calibrated MAP tables according to the required operating parameters. It subsequently generates a current signal to control the solenoid valve, activating the injector to perform fuel injection.

This research focuses on realizing the closed-loop control of the fuel injection volume based on estimated injection information, so as to improve the control accuracy and anti-disturbance performance of the fuel injection process. The overall scheme of the fuel injection closed-loop control system is shown in Figure 1.

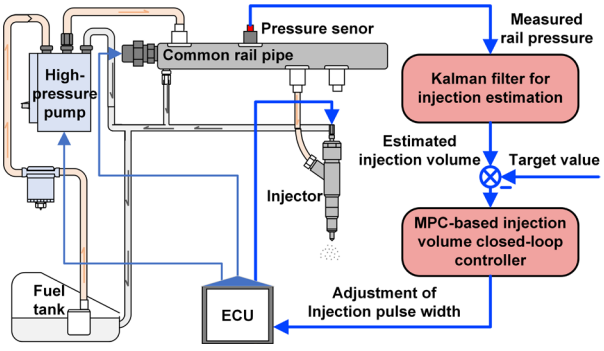

Figure 1. Schematic diagram of the fuel injection volume closed-loop control system.

First, the real-time collected common rail pressure signal *p* is input into the injection estimation Kalman filter, utilizes the instantaneous rail pressure fluctuation to estimate the fuel injection information [15]. The design process of the Kalman filter is shown in Figure 2. It uses the difference between the measured and estimated rail pressure to carry out feedback correction and rolling optimization of the injection process state, thereby achieving the real-time optimal estimation of the injection rate. The estimated injection rate is then integrated during the injection period to obtain the injection volume:

$$\hat{V}_{\mathrm{inj}} = \sum_{k=k_0}^{k_n} \hat{Q}_{\mathrm{inj}}^{+}(k) \cdot \Delta t \tag{1}$$

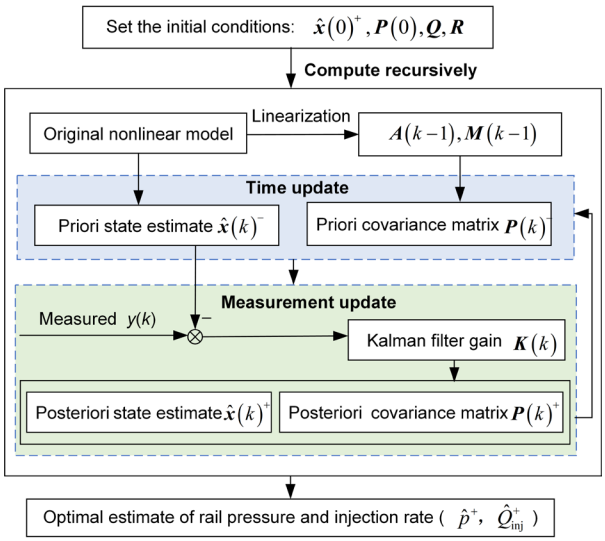

Figure 2. Design process of the injection estimation Kalman filter.

Next, with the estimated injection volume as the feedback and the target volume as the reference input, the closed loop control system is formed. The difference between the estimated and target injection volume is input into the MPC controller, which calculates the adjustment in the injection pulse width. According to the current injection pulse width, the solenoid valve controls the opening and closing timing of the needle valve in the injector, ensuring the system's injection volume matches the desired value.

This paper primarily focuses on the design and optimization research of the MPC-based closed-loop control method for fuel injection and provides an in-depth discussion of the performance of the closed-loop control system.

3 MPC-BASED INJECTION VOLUME CLOSED-LOOP CONTROL DESIGN

Since the MPC is a model-based control method, it requires a high level of accuracy for the system model. This section initially introduces the development of the fuel injection volume model and subsequently addresses the optimization of model parameters to enhance the model accuracy across

multiple conditions. Based on this model, the design of the MPC controller is then performed. Additionally, considering the constraints on the actuator, the predictive controller is optimized to accommodate these limitations.

3.1 Fuel Injection Prediction Model

Simplifying the injection process as a first-order inertial system, the mathematical model between the injection volume V_{inj} and the injection pulse width *IPW* is established. Taking *IPW* as input and V_{inj} as output, the system is modeled as:

$$G(s) = \frac{K}{Ts+1} \tag{2}$$

where K is the proportion coefficient, T is the time constant.

For a given rail pressure condition, the proportion coefficient K can be regarded as a constant. However, the value of K will change with different rail pressures. To address the issue of model parameter matching under conditions with large variations in rail pressure, it is necessary to identify the variation of K and obtain the following expression:

$$K\left(p_{ss}\right) = c_0 p_{ss} + c_1 \tag{3}$$

where p_{ss} is the target rail pressure. c_0 and c_1 are the model coefficients, which need to be identified using data from different pressure conditions.

Selecting the injection volume as the state variable x_m, the injection pulse width as the control variable u, a discrete-time state space model of the system is obtained with Δt as the discrete sampling interval:

$$\begin{aligned} x_m(k+1) &= A_m \cdot x_m(k) + B_m(k) \cdot u(k) \\ y(k) &= C_m \cdot x_m(k) \end{aligned} \tag{4}$$

where A_m=1-$\Delta t/T$, B_m=$\Delta t \cdot K(p_{ss})/T$, C_m=1. B_m is time-varying and changes with the target rail pressure conditions. During the actual operation, the model accuracy will be improved by updating the model parameters in real time.

To minimize the steady-state error and overshoot of the controller, this study employs an incremental model in the design process. To calculate the increment of the control signal, let:

$$\boldsymbol{x}(k) = \begin{bmatrix} x_m(k+1) - x_m(k) \\ y(k) \end{bmatrix}, \ \Delta u(k) = u(k+1) - u(k)$$

Thus, an augmented model is obtained:

$$\begin{aligned} \boldsymbol{x}(k) &= \boldsymbol{A} \cdot \boldsymbol{x}(k) + \boldsymbol{B}(k) \cdot \Delta u(k) \\ y(k) &= \boldsymbol{C} \cdot \boldsymbol{x}(k) \end{aligned} \tag{5}$$

where $\boldsymbol{A} = \begin{bmatrix} A_m & 0 \\ C_m A_m & 1 \end{bmatrix}, \boldsymbol{B} = \begin{bmatrix} B_m \\ C_m B_m \end{bmatrix}, \boldsymbol{C} = \begin{bmatrix} 0 & 1 \end{bmatrix}$.

3.2 Design of MPC with Constraints

MPC utilizes the predictive model to forecast the future dynamic behavior of the system under specific control action and iteratively solves for the current optimal control input based on performance criteria. The detailed design process is described as follows.

3.2.1 Output prediction

Define the prediction horizon as N_p and the control horizon as N_c. At sampling instant k, with available information $x(k)$, the system output over the next N_p steps within the control horizon N_c is computed according to Equation 5:

$$\begin{aligned} y(k+1|k) &= \boldsymbol{CA}\boldsymbol{x}(k) + \boldsymbol{CB}\Delta u(k) \\ y(k+2|k) &= \boldsymbol{CA}\boldsymbol{x}(k+1|k) + \boldsymbol{CB}\Delta u(k+1) \\ &= \boldsymbol{CA}^2\boldsymbol{x}(k) + \boldsymbol{CA}^2\boldsymbol{B}\Delta u(k) + \boldsymbol{CB}\Delta u(k+1) \\ &\vdots \\ y(k+N_p|k) &= \boldsymbol{CA}^{N_p}\boldsymbol{x}(k) + \boldsymbol{CA}^{N_p-1}\boldsymbol{B}\Delta u(k) \\ &\quad + \cdots + \boldsymbol{CA}^{N_p-N_c}\boldsymbol{B}\Delta u(k+N_c-1) \end{aligned} \tag{6}$$

Define the predicted output sequence $\boldsymbol{Y}(k)$ and the future control increment sequence $\Delta\boldsymbol{U}(k)$:

$$\boldsymbol{Y} = \begin{bmatrix} y(k+1|k) & y(k+2|k) & \cdots & y(k+N_p|k) \end{bmatrix}^{\mathrm{T}}$$

$$\Delta\boldsymbol{U}(k) = \begin{bmatrix} \Delta u(k) & \Delta u(k+1) & \cdots & \Delta u(k+N_c-1) \end{bmatrix}^{\mathrm{T}}$$

This yields the predicted output equation as:

$$\boldsymbol{Y} = \boldsymbol{F}\boldsymbol{x}(k) + \boldsymbol{\Phi}\Delta\boldsymbol{U} \tag{7}$$

where the matrices $\boldsymbol{F}$ and $\boldsymbol{\Phi}$ are

$$F = \begin{bmatrix} CA & CA^2 & CA^3 & \cdots & CA^{N_p} \end{bmatrix}$$

$$\Phi = \begin{bmatrix} CB & 0 & 0 & \cdots & 0 \\ CAB & CB & 0 & \cdots & 0 \\ CA^2B & CAB & CB & \cdots & 0 \\ \vdots & \vdots & \vdots & & \vdots \\ CA^{N_p-1}B & CA^{N_p-2}B & CA^{N_p-3}B & \cdots & CA^{N_p-N_c}B \end{bmatrix}$$

3.2.2 Rolling optimization

A quadratic cost function is employed in the MPC as an optimization performance index, which considers all the control objectives. The aim of this study is to achieve fast and stable tracking of fuel injection output. Additionally, the control input variation should be minimized to avoid overshoot. Therefore, considering both the future output tracking error and the control increment, the quadratic cost function is defined as:

$$J = \left(\boldsymbol{R}_s - \boldsymbol{Y}\right)^{\mathrm{T}} \boldsymbol{Q}\left(\boldsymbol{R}_s - \boldsymbol{Y}\right) + \Delta \boldsymbol{U}^{\mathrm{T}} \boldsymbol{R} \Delta \boldsymbol{U} \tag{8}$$

where $\boldsymbol{R}_\mathbf{s}$ is a column vector formed by the given injection reference value $r(k)$, and $\boldsymbol{R}_\mathbf{s}^{\mathbf{T}} = r(k)$ [1 1 … 1]$_{1\times Np}$. $\boldsymbol{Q}$ is a diagonal matrix in the form that $\boldsymbol{Q}=q_w \boldsymbol{I}_{Np\times Np}$ where q_w is the weighting factor of the output error. $\boldsymbol{R}$ is also a diagonal matrix and $\boldsymbol{R}=r_w \boldsymbol{I}_{Nc\times Nc}$ where r_w is the weighting factor of the control increment.

Substitute the predicted output Equation 7 into Equation 8:

$$\begin{aligned} J = &\left(\boldsymbol{R}_s - \boldsymbol{F}\boldsymbol{x}(k)\right)^{\mathrm{T}} \boldsymbol{Q}\left(\boldsymbol{R}_s - \boldsymbol{F}\boldsymbol{x}(k)\right) \\ &-2\Delta \boldsymbol{U}^{\mathrm{T}} \boldsymbol{\Phi}^{\mathrm{T}} \boldsymbol{Q}\left(\boldsymbol{R}_s - \boldsymbol{F}\boldsymbol{x}(k)\right) + \Delta \boldsymbol{U}^{\mathrm{T}}\left(\boldsymbol{\Phi}^{\mathrm{T}} \boldsymbol{Q} \boldsymbol{\Phi} + \boldsymbol{R}\right)\Delta \boldsymbol{U} \end{aligned} \tag{9}$$

By minimizing this cost function (9), the optimal control sequence without constraints is obtained:

$$\Delta \boldsymbol{U} = (\boldsymbol{\Phi}^{\mathrm{T}} \boldsymbol{Q} \boldsymbol{\Phi} + \boldsymbol{R})^{-1} \boldsymbol{\Phi}^{\mathrm{T}} \boldsymbol{Q}(\boldsymbol{R}_{\mathrm{s}} - \boldsymbol{F}\boldsymbol{x}(k)) \tag{10}$$

3.2.3 Optimal control with constraints

In practical system operation, there usually exists actuator constraints. Due to the limitations of the injection pulse width, constraints are required for both the control signal and its increments in this study.

The control signal and its increment constraint range are:

$$u_{\min} \le u \le u_{\max} \tag{11}$$

$$\Delta u_{\min} \le \Delta u \le \Delta u_{\max} \tag{12}$$

where $u_{\max}$ and $u_{\min}$ represent the maximum and minimum values of the control signal, respectively. $\Delta u_{\max}$ and $\Delta u_{\min}$ denote the upper and lower bounds of the control increment, respectively.

Since only the first term $\Delta u(k)$ of the control sequence $\Delta \boldsymbol{U}(k)$ is applied in actual control, constraints are only imposed on the first term of $\Delta \boldsymbol{U}$ to reduce computational load.

All constraints are uniformly expressed in the following matrix form:

$$\boldsymbol{A}_{\mathrm{cons}} \Delta \boldsymbol{U} \le \boldsymbol{b} \tag{13}$$

where $\boldsymbol{A}_{\mathrm{cons}}$ and $\boldsymbol{b}$ are

$$\boldsymbol{A}_{\mathrm{cons}} = \begin{bmatrix} 1 & 0 & \cdots & 0 \\ -1 & 0 & \cdots & 0 \\ 1 & 0 & \cdots & 0 \\ -1 & 0 & \cdots & 0 \end{bmatrix}_{4\times N_{\mathrm{c}}}, \boldsymbol{b} = \begin{bmatrix} \Delta u_{\max} \\ -\Delta u_{\min} \\ u_{\max} - u(k-1) \\ -u_{\min} + u(k-1) \end{bmatrix}$$

Let $\boldsymbol{E} = \boldsymbol{\Phi}^{\mathrm{T}} \boldsymbol{Q} \boldsymbol{\Phi} + \boldsymbol{R}$ and $\boldsymbol{F}_{\mathrm{n}} = \boldsymbol{\Phi}^{\mathrm{T}} \boldsymbol{Q} \boldsymbol{F} \boldsymbol{x}(k_i) - \boldsymbol{\Phi}^{\mathrm{T}} \boldsymbol{Q} \boldsymbol{R}_{\mathrm{s}}$, and simplify the term in Equation 8 that is independent of ΔU. The resulting expression is as follows:

$$J = \Delta \boldsymbol{U}^{\mathrm{T}} \boldsymbol{E} \Delta \boldsymbol{U} + 2\Delta \boldsymbol{U}^{\mathrm{T}} \boldsymbol{F}_{\mathrm{n}} \tag{14}$$

By introducing the Lagrange multiplier $\boldsymbol{\lambda}$, Equations 13 and 14 are formulated as a standard quadratic programming problem with respect to $\Delta \boldsymbol{U}$:

$$\min_{\Delta U} J = \Delta \boldsymbol{U}^{\mathrm{T}} \boldsymbol{E} \Delta \boldsymbol{U} + 2\Delta \boldsymbol{U}^{\mathrm{T}} \boldsymbol{F}_{\mathrm{n}} + \boldsymbol{\lambda}\left(\boldsymbol{A}_{\mathrm{cons}} \Delta \boldsymbol{U} - \boldsymbol{b}\right) \tag{15}$$

By solving this quadratic programming problem, the optimal control sequence $\Delta \boldsymbol{U}$ with constraints is determined:

$$\boldsymbol{\lambda} = -\left(\boldsymbol{A}_{\mathrm{cons}} \boldsymbol{E}^{-1} \boldsymbol{A}_{\mathrm{cons}}^{\mathrm{T}}\right)^{-1}\left(\boldsymbol{b} + \boldsymbol{A}_{\mathrm{cons}} \boldsymbol{E}^{-1} \boldsymbol{F}_{\mathrm{n}}\right) \tag{16}$$

$$\Delta \boldsymbol{U} = -\boldsymbol{E}^{-1} \boldsymbol{F}_{\mathrm{n}} - \boldsymbol{E}^{-1} \boldsymbol{A}_{\mathrm{cons}}^{\mathrm{T}} \boldsymbol{\lambda} = \Delta \boldsymbol{U}_0 - \boldsymbol{E}^{-1} \boldsymbol{A}_{\mathrm{cons}}^{\mathrm{T}} \boldsymbol{\lambda} \tag{17}$$

where the first term $\Delta \boldsymbol{U}_\mathbf{0}$ represents the global optimal solution that minimizes the original cost function J with no constraint. The second term of Equation 17 is the correction term arising from the constraint conditions.

The $\Delta u(k)$ of the optimal $\Delta \boldsymbol{U}$ is taken as the control increment at moment k, which is applied to the control system to form the closed-loop control. Consequently, the control signal at the next moment is obtained:

$$u\left(k+1\right) = u\left(k\right) + \Delta u\left(k\right) \tag{18}$$

3.3 Overall Structure of the Injection Closed-loop Control Algorithm

The structure of the MPC algorithm designed in this section is presented in Figure 3:

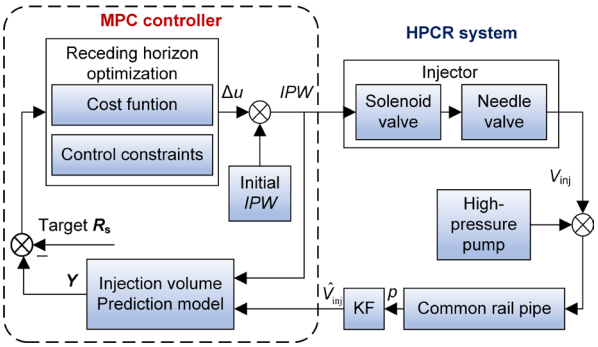

Figure 3. Flowchart of MPC-based injection volume closed-loop control.

Besides, the ratio between the weighting matrices ***Q*** and ***R*** should be appropriately selected during the design process, which significantly influences the stability and response speed of the closed-loop control.

4 IMPLEMENTATION AND RESULTS ANALYSIS

In this section, the implementation process of the proposed injection closed-loop control method in a practical system is described first. Subsequently, the impact of the weighting matrices in the cost function on control performance is discussed. To verify the effectiveness of the designed controller, the anti-disturbance and robustness of the closed-loop control system are investigated under different conditions.

4.1 Implementation

The MPC-based closed-loop control system of fuel injection volume proposed in this paper utilizes the rail pressure fluctuation to estimate the fuel injection information. The estimated injection volume is then used as feedback, and the designed MPC controller computes the pulse width control input, thereby achieving closed-loop control of the fuel injection volume. To conduct research on fuel injection estimation and control, a high-pressure common rail test bench is built, which is shown in Figure 4.

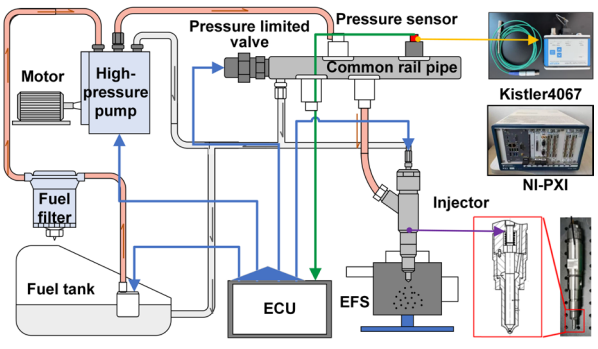

Figure 4. Schematic diagram of HPCR platform.

The experimental platform consists of a common rail pipe, a high-pressure fuel pump, solenoid valve-type injectors, and high-pressure fuel tubes. Additionally, it is equipped with an electronic control unit (ECU) and several measurement devices, which enables the control and measurement of the rail pressure and injection parameters.

Before the proposed method is implemented in real-time, it is necessary to identify the model parameters for the specific system, which requires a large amount of data for various operating conditions. Therefore, a simulation model of the common rail system is established using Amesim based on the experimental bench parameters, as shown in Figure 5. The model has been validated using experimental data with the simulation errors for injection parameters and rail pressure less than 5%, which demonstrates its high accuracy. It can provide support for the model parameter identification and method validation.

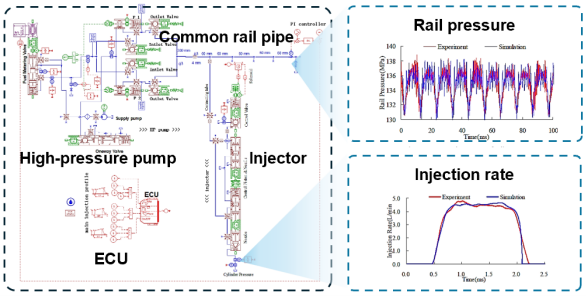

Figure 5. HPCR system Amesim simulation model.

In this section, a detailed description of the parameter identification and real-time calculation processes for this system will be provided.

4.1.1 Parameter identification

Before real-time implementation, the Kalman filter and controller related model parameters need to be identified. The parameter identification for the Kalman filter has been presented in the literature [15], and high estimation accuracy has been demonstrated using simulation and experimental data. This section primarily focuses on identifying the parameters $K(p_{ss})$ and T in the fuel injection model (4) from Section 3.1.

K is the proportionality coefficient between the injection volume output and the injection pulse width. The inertia time constant T is defined as the time required for the output response to reach 0.632 times the steady-state value. The values of K and T are determined based on the fuel injection volume data obtained from the Amesim model under different rail pressure and injection pulse width conditions. Fuel injection volume data for several operating conditions are shown in Figure 6,

while the detailed calculation results are given in Table 1.

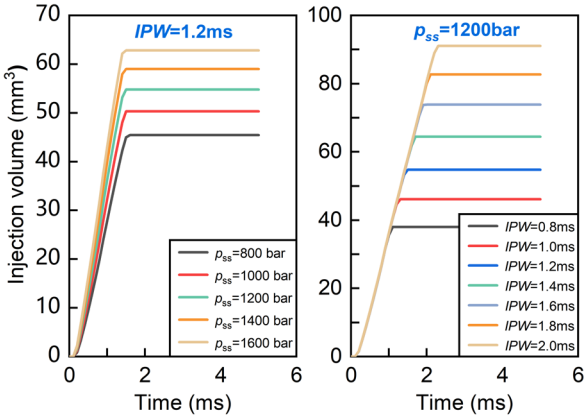

Figure 6. Injection volume data at various operating conditions.

Table 1. Identified value of *K* and *T*.

p_{ss} (bar)	*IPW* (ms)	*K* (mm³/ms)	*T* (s)
1000	0.8	43.75	0.00065
	1.2	42.05	0.00088
	1.6	42.43	0.00112
	2.0	41.57	0.00136
1200	0.8	47.5	0.00064
	1.2	45.7	0.00087
	1.6	46.2	0.00114
	2.0	45.5	0.00139
1400	0.8	51.29	0.00062
	1.2	49.20	0.00086
	1.6	49.8	0.00123
	2.0	48.8	0.00147

It is evident that, due to the brief duration of the fuel injection process, the *T* values under different operating conditions exhibit minimal variation and can be approximated as a constant. Taking the average as the value of *T*, it is 0.0011 s. In addition, under a given pressure, the *K* remains relatively stable. However, it exhibits significant variation across different pressures. The identified expression for the variation of *K* with pressure is:

$$K(p_{ss}) = 0.1876 p_{ss} + 23.542 \tag{19}$$

4.1.2 Real-time control calculation

This section describes the real-time computation process for the MPC closed-loop control. The calculation of real-time optimal control signals requires the matrices $\boldsymbol{R}_s$, $\boldsymbol{\Phi}$, and $\boldsymbol{F}$. After setting the initial target rail pressure, the desired fuel injection volume, control horizon, and prediction horizon parameters, these matrices are solved according to the formulas given in Section 3.2. Among them, $\boldsymbol{R}_s$ and $\boldsymbol{\Phi}$ only need to be solved offline, while $\boldsymbol{F}$ contains the variable p_{ss}, which requires real-time updates when the rail pressure conditions change.

Moreover, the optimal control computation with constraints involves solving a quadratic programming (QP) problem, and the speed of this process determines the step size for each iteration in the real-time control process. To address this, the Hildreth method is employed in this study. The Hildreth method is an element-by-element solution algorithm that transforms the complex quadratic programming problem into a series of linear programming problems, avoiding matrix inversion operations, thereby ensuring the efficiency and stability of the system in real-time applications (with an average computation time of 2.15e-3 seconds).

The process begins by calculating the global optimal solution $\Delta\boldsymbol{U}_0$ based on Equation 17 and checking whether it satisfies the constraint conditions. If not, the Lagrange multiplier $\boldsymbol{\lambda}$ is iteratively computed until convergence, at which point the constrained optimal solution is obtained:

$$\begin{aligned} \lambda_i^{m+1} &= \max\left(0, w_i^{m+1}\right) \\ w_i^{m+1} &= -\frac{1}{h_{ii}}\left[k_i + \sum_{j=1}^{i-1} h_{ij}\lambda_i^{m+1} + \sum_{j=i+1}^{n} h_{ij}\lambda_i^{m}\right] \end{aligned} \tag{20}$$

where h_{ij} is the ijth element in $\boldsymbol{A}_{cons}\boldsymbol{E}^{-1}\boldsymbol{A}_{cons}^{T}$, k_i is the ith element in $\boldsymbol{b}+\boldsymbol{A}_{cons}\boldsymbol{E}^{-1}\boldsymbol{F}_n$.

Thus, the optimal control sequence $\Delta\boldsymbol{U}$ under constraints is obtained, and the first element of this sequence is applied to the system for real-time control.

4.1.3 Closed-loop control implementation and control parameter design

To analyze the control performance and verify its effectiveness, this study employs co-simulation of the injection volume closed-loop control system. Specifically, the designed MPC-based closed-loop controller is developed in Simulink and co-simulated with the AMESim model. Figure 7 illustrates the schematic diagram of data interaction in the co-simulation.

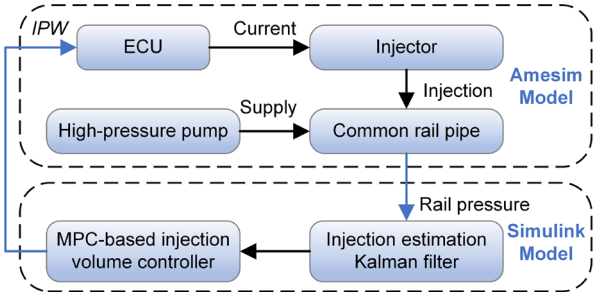

Figure 7. Schematic diagram of Co-simulation data interaction of the fuel injection volume closed-loop control.

During the controller design process, it is observed that the ratio of the error weighting matrix ***Q*** to the control increment weighting matrix ***R*** significantly influences the controller's performance. This section investigates the impact of this parameter on the control performance.

The injection pulse width constraints are set as: $0 \le u \le 2$ and $-0.5 \le \Delta u \le 0.5$. The operation time is 0.6 seconds with a sampling interval T_s = 0.1 ms, and the injection interval is 15 ms. The target fuel injection volume is initially set to 64 mm³, with a sudden change to 74 mm³ at 0.3 seconds. With q_w in ***Q*** fixed at 0.1, r_w in ***R*** is varied to 1, 10, 100, and 1000. The control input and fuel injection volume variation curves are shown in Figure 8.

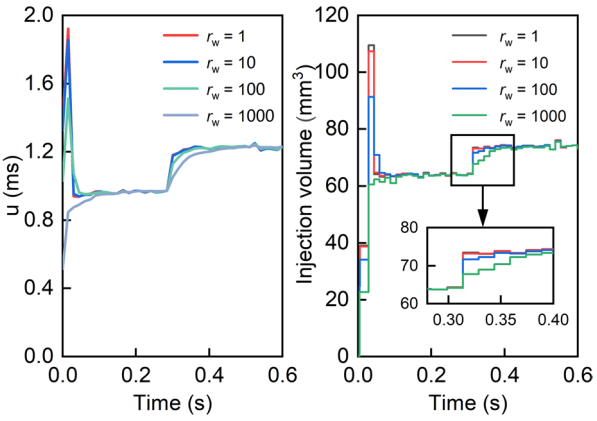

Figure 8. Control and output signals under different control parameters.

It is seen that as the ratio of ***Q*** and ***R*** decreases, the fuel injection adjustment response becomes slower. Conversely, a larger ratio leads to a faster response but increased overshoot. After considering the trade-off between response speed and overshoot, the final chosen control parameters are q_w = 0.1 and r_w = 300.

4.2 Anti-disturbance Performance Analysis

To verify the anti-disturbance performance of the designed control system, this section conducts an analysis under two conditions: variable target fuel injection volume condition and fixed working condition with disturbed control signals.

Figure 9 shows the comparison between the actual and target injection volume when the target value changes from 64 mm³ to 74 mm³ at 0.3 s. The results indicate that when the reference signal undergoes a step change, the control system is able to regulate the fuel injection volume within 2% error in 3-4 injection cycles.

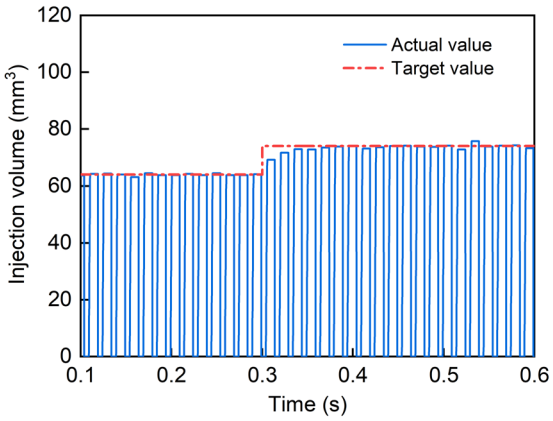

Figure 9. Fuel injection output under variable target fuel injection volume condition.

Figure 10 illustrates the comparison between the actual and target fuel injection volume when the pulse width signal is subjected to a brief disturbance of -0.2 ms between 0.3s and 0.4s. Figure 11 shows the control performance after a continuous disturbance of -0.2 ms is applied to the control signal starting at 0.3s.

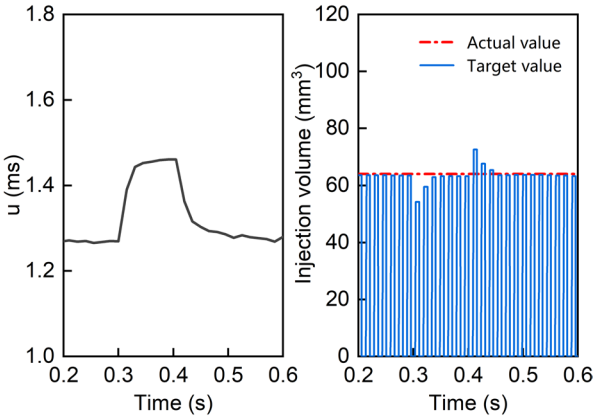

Figure 10. Control signal and injection volume output under brief disturbance.

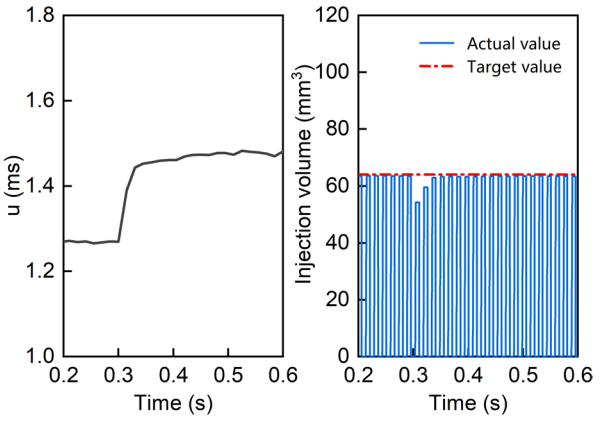

Figure 11. Control signal and injection volume output under continuous disturbance.

When the control signal is disturbed, under the action of this controller, the actual fuel injection volume is adjusted back to near the target value after 2-3 injection cycles.

4.3 Robustness Analysis

This section verifies the robustness of the control system under varying rail pressure and speed conditions while maintaining the same control parameters.

Figures 12 and 13 illustrate the control results of the injection closed-loop system when the rail pressure changes at 0.3s.

The following subfigure (a) shows the comparison between the actual and target fuel injection volume results. Subfigure (b) gives the adjustment of the injection pulse width control signal. And subfigure (c) is the variation of the instantaneous rail pressure.

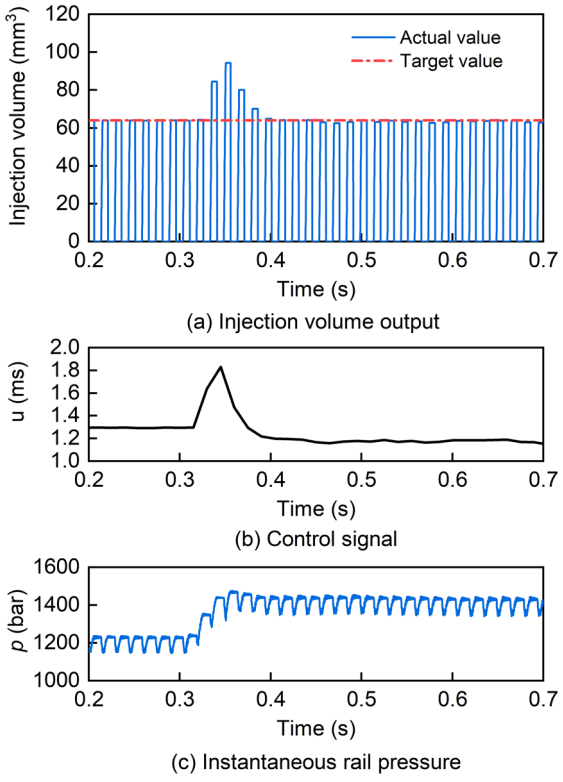

Figure 12. Injection control results under pressure rise condition (1200 → 1400 bar).

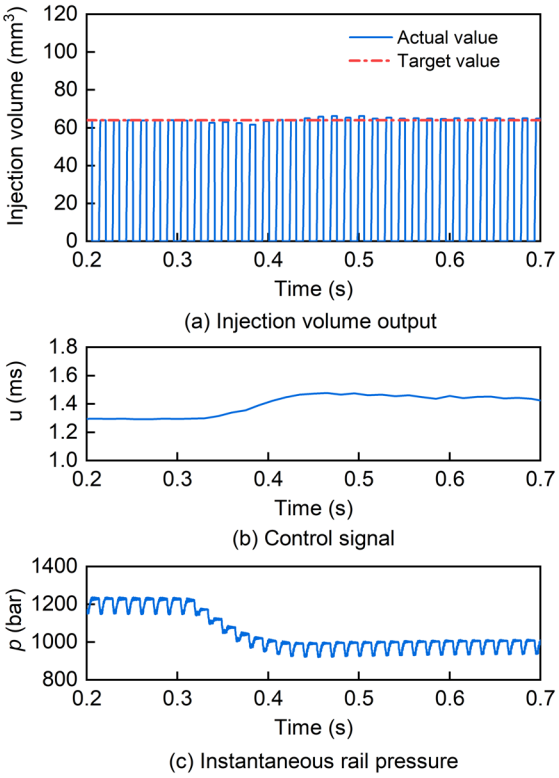

Figure 13. Injection control results under pressure drop condition (1200 → 1000 bar).

Figure 14 demonstrates the comparison of the fuel injection outputs at different engine speeds.

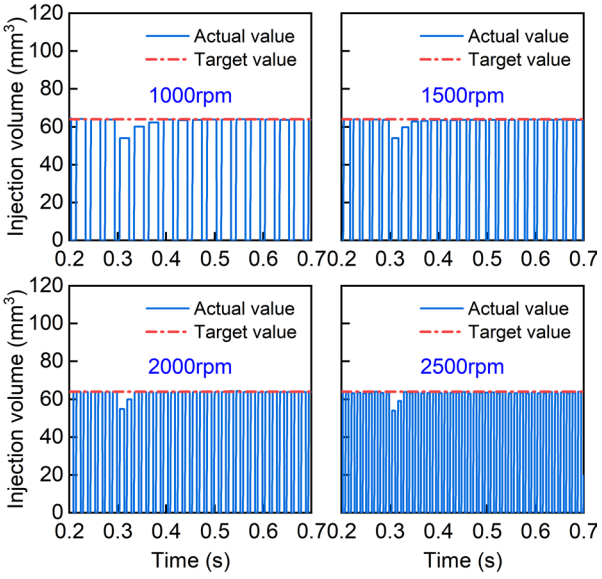

Figure 14. Injection control results under different engine speeds

The results indicate that, even when the common rail pressure or engine speed changes, the fuel injection volume closed-loop controller designed in

this study maintains good control performance without altering the control parameters.

5 CONCLUSIONS

The injection performance of the high-pressure common rail (HPCR) fuel injection system determines the combustion efficiency and emission levels. Accurate and stable control of fuel injection is crucial for enhancing engine performance and reducing emissions. However, due to the complex hydrodynamic effects in HPCR systems, the current open-loop control method based on MAP tables struggles to ensure precise fuel injection. To improve the control accuracy of the fuel injection process, this study has proposed an MPC-based closed-loop control method for fuel injection volume, which utilizes the real-time injection information estimated by Kalman filter as feedback. The control performance of this method has been thoroughly analyzed. The main conclusions of this study are summarized as follows:

1 Based on the control mechanism of the injection process, and considering the model parameter matching under varying operating conditions, a fuel injection prediction model suitable for different conditions was developed. This model provides a solid foundation for the design of the model predictive controller.

2 Considering the constraints on injection pulse width control signal, a constrained MPC controller was studied and designed. To enhance the computational efficiency in practical applications, the Hildreth algorithm was employed for real-time optimal control signal computation. Furthermore, the impact of the weight matrices in the cost function was investigated.

3 To validate the feasibility and effectiveness of the proposed method, an Amesim/Simulink co-simulation platform was constructed. The performance of the designed closed-loop fuel injection volume control system was comprehensively analyzed. The results demonstrate that the MPC-based closed-loop controller exhibits a strong anti-disturbance capability and robustness. In the presence of external disturbances, the fuel injection deviation can be controlled within 3% of the target value after 2-3 injection cycles. Moreover, when engine operating conditions change, the actual fuel injection volume quickly converges to the set target value without adjusting controller parameters.

6 ACKNOWLEDGMENTS

The authors gratefully acknowledge the financial support of the National Natural Science Foundation of China (51879059, 52071106).

7 REFERENCES AND BIBLIOGRAPHY

[1] Costagliola, M.A., Costabile, M. and Prati, M.V. 2018. Impact of road grade on real driving emissions from two Euro 5 diesel vehicles, *Applied Energy*, 231:586-593.

[2] Liu, L., Peng, Y., Zhang, W. and Ma, X. 2023. Concept of rapid and controllable combustion for high power-density diesel engines, *Energy Conversion and Management*, 276:116529.

[3] Sidhu, M. S., Roy, M. M., and Wang, W. 2018. Glycerine emulsions of diesel-biodiesel blends and their performance and emissions in a diesel engine, *Applied Energy*, 230, 148-159.

[4] Hu, Y., Yang, J., & Hu, N. 2021. Experimental study and optimization in the layouts and the structure of the high-pressure common-rail fuel injection system for a marine diesel engine, *International Journal of Engine Research*, 22(6): 1850-1871.

[5] Gupta, V. K., Zhang, Z., and Sun, Z. 2011. Modeling and control of a novel pressure regulation mechanism for common rail fuel injection systems, *Applied Mathematical Modelling*, 35(7), 3473-3483.

[6] Ferrari, A., and Paolicelli, F. 2017. An indirect method for the real-time evaluation of the fuel mass injected in small injections in Common Rail diesel engines. *Fuel*, 191, 322-329.

[7] Voigt, P., Schiffgens, H.J., Daveau, C., Ogé, J.C., Béduneau, J.L., Meissonier, G., Tapin, C. and Lalé, X. 2017. Delphi injector closed loop control strategy using the “Switch” technology for Diesel passenger cars–injector hardware. *Tagung Diesel- und Benzindirekteinspritzung 2016: Inklusive Gaseinblasung*, Wiesbaden, 41-66.

[8] Wintrich, T., Rothe, S., Bucher, K., and Hitz, H. J. 2018. Diesel injection system with closed-loop control. *MTZ worldwide*, 79(9): 54-59.

[9] Ferrari, A., Novara, C., Paolucci, E., Vento, O., Violante, M., and Zhang, T. 2018. Design and rapid prototyping of a closed-loop control strategy of the injected mass for the reduction of CO2, combustion noise and pollutant emissions in diesel engines, *Applied Energy*, 232: 358-367.

[10] Ferrari, A., Novara, C., Vento, O., Violante, M., and Zhang, T. 2023. A novel fuel injected mass feedback-control for single and multiple injections in direct injection systems for CI engines, *Fuel*, 334: 126670.

[11] Krogerus, T., Hyvönen, M., and Huhtala, K. 2018. Analysis of common rail pressure signal of dual-fuel large industrial engine for identification of injection duration of pilot diesel injectors, *Fuel*, 216, 1-9.

[12] Payri, F., Luján, J. M., Guardiola, C., and Rizzoni, G. 2006. Injection diagnosis through common-rail pressure measurement. *Proceedings of the Institution of Mechanical Engineers, Part D: Journal of Automobile Engineering*, 220(3): 347-357.

[13] Krogerus, T. R., Hyvönen, M. P., and Huhtala, K. J. 2016. A survey of analysis, modeling, and diagnostics of diesel fuel injection systems, *Journal of Engineering for Gas Turbines and Power*, 138(8): 081501.

[14] Krogerus, T. R., and Huhtala, K. J. 2018. Diagnostics and identification of injection duration of common rail diesel injectors, *Open Engineering*, 8(1): 1-6.

[15] Fei, H., Liu, B., Wang, L., and Fan, L. 2023. Optimal estimation of injection rate for high-pressure common rail system using the extended Kalman filter. *Measurement*, 220: 113385.

[16] Liu, B., Fei, H., Wang, L., Fan, L., and Yang, X. 2024. Real-time estimation of fuel injection rate and injection volume in high-pressure common rail systems. *Energy*, 298: 131386.

[17] Wang, L. 2009. *Model predictive control system design and implementation using MATLAB*. London: springer.

[18] Yang, L., Wang, W., Yang, C., Du, X., Liu, W., Zha, M., and Liang, B. 2024. A self-triggered MPC strategy with adaptive prediction horizon for series hybrid electric powertrains. *IEEE Transactions on Industrial Informatics*,1-10.

[19] Liu, W., Gao, Y., You, Y., Jiang, C., Hua, T., & Xia, B. 2024. Nonlinear model predictive control (NMPC) of diesel oxidation catalyst (DOC) outlet temperature for active regeneration of diesel particulate filter (DPF) in diesel engine. *Energy*, 293: 130658.

[20] Ahmed, O. Y., Middleton, R. J., Tran, V., Weng, A., Stefanopoulou, A. G., Kim, K. S., & Kweon, C. B. M. 2022. Model predictive control of combustion phasing in compression ignition engines by coordinating fuel injection timing and ignition assist. *IFAC-PapersOnLine*, 55(24): 90-96.

[21] Sankar, G. S., Shekhar, R. C., Manzie, C., Sano, T., & Nakada, H. 2019. Fast calibration of a robust model predictive controller for diesel engine airpath. *IEEE Transactions on Control Systems Technology*, 28(4): 1505-1519.

8 CONTACT

Hongzi Fei
Professor, Ph.D.

College of Power and Energy Engineering
Harbin Engineering University
145 Nantong Street, Nangang District, Harbin 150001, Cnina

Tel: +86 13845067317
Email: fhz@hrbeu.edu.cn